Peg-Free Hand Shape Verification Using High Order Zernike Moments

Gholamreza Amayeh, George Bebis, Ali Erol, and Mircea Nicolescu
Computer Vision Laboratory, University of Nevada, Reno, NV 89557
{amayeh, bebis, aerol, mircea}@cse.unr.edu

Abstract

Hand-based verification is a key biometric technology with a wide range of potential applications both in industry and government. The focus of this work is on improving the efficiency, accuracy, and robustness of hand-based verification. In particular, we propose using high-order Zernike moments to represent hand geometry, avoiding the more difficult and prone to errors process of hand-landmark extraction (e.g., finding finger joints). The proposed system operates on 2D hand silhouette images acquired by placing the hand on a planar lighting table without any guidance pegs, increasing the ease of use compared to conventional systems. Zernike moments are powerful translation, rotation, and scale invariant shape descriptors. To deal with several practical issues related to the computation of high-order Zernike moments including computational cost and lack of accuracy due to numerical errors, we have employed an efficient algorithm that uses arbitrary precision arithmetic, a look-up table, and avoids recomputing the same terms multiple times [2]. The proposed hand-based authentication system has been tested on a database of 40 subjects illustrating promising results. Qualitative comparisons with state of the art systems illustrate comparable of better performance.

1. Introduction

Recently, there has been increased interest in developing biometrics-based authentication systems which has led to intensive research in fingerprint, face, hand, ear, and iris recognition. Each biometric has its strength and weakness depending on the application and its requirements. Hand-based authentication, which is the topic of this study, is among the oldest live biometrics-based authentication modalities. The geometry of the hand contains relatively invariant features of an individual. The existence of several hand-based authentication commercial systems and patents indicate the effectiveness of this type of biometric. Hand-based verification systems are usually employed in small-scale person authentication applications due to the fact that geometric features of the hand (e.g., finger length/width, area/size of the palm) are not as distinctive as fingerprint or iris features.

There are several reasons for developing hand-based authentication systems. First, hand shape can be easily captured in a relatively user friendly manner by using conventional CCD cameras. Second, this technology is more acceptable by the public in daily life mainly because it lacks a close connection to forensic applications. Finally, there has been some interest lately in fusing different biometrics to increase system performance [15, 9]. The ease of use and acceptability of hand-based biometrics make hand shape a good candidate in these heterogeneous systems.

Although hand-based live verification has a long history and a considerable market share [1], most studies addressing enhancements of this technology are rather recent [7]. Increases in computing power and advances in computer vision and pattern recognition are expected to facilitate the implementation of easier to use systems with higher accuracy. Removal of pegs, to improve convenience, and use of more principled feature extraction techniques to capture the shape of the hand in more detail represent promising research directions in this area.

The focus of this work is on improving the efficiency, accuracy, and robustness of hand-based verification. One can imagine utilizing various shape descriptors to provide a more powerful representation of the shape of the hand, replacing the conventional geometric features. In this study, we present the design and implementation of a hand-based verification system using high-order Zernike moments. The system operates on 2D hand silhouette images acquired by placing the hand on a planar lighting table without any guidance pegs, therefore, increasing the ease of use. Moreover, it does not require extracting any landmarks on the hand (e.g., finding finger joints), a process which could be prone to errors.

Zernike moments, have been employed in a wide range of applications in image analysis, and object recognition [21]. They are quite attractive for representing hand shape information due to having minimal redundancy (i.e., orthogonal basis functions [19]), and being invariant with re-

spect to translation, rotation, and scale, as well as robust to noise [20]. In most applications, however, their use has been limited to low-orders only or small low-resolution images due to high computational requirements and lack of accuracy due to numerical errors. Although there exist some fast algorithms that rely on approximate polar coordinate transformations [13, 3, 5], we could not obtain satisfactory results in the context of our application due to the approximations involved (i.e., lack of accuracy).

Using Zernike moments for hand-based authentication requires fast computation of high-order moments as accurately as possible, in order to capture the details of the hand shape. To deal with these requirements, we are employing an efficient algorithm previously developed in [2] that reduces computation cost without sacrificing accuracy. To preserve accuracy, this algorithm avoids any form of coordinate transformations and it uses arbitrary precision arithmetic. To reduce computational complexity, it avoids recomputing the same terms multiple times and uses a look-up table to save computations. It should be mentioned that high-order Zernike moments are usually more sensitive to noise, however, this is not an issue in our application since the amount of noise present in our data is rather low due to the acquisition process employed (see Section 3). We demonstrate the performance of the proposed hand-based authentication system on a database of 40 subjects with 10 images per subject. Qualitative comparisons illustrate that the proposed approach performs comparable or better than state of the art systems reported in the literature.

The rest of the paper is organized as follows: in the next Section, we present a brief literature review on hand-based authentication systems. Section 3, contains the details of the image acquisition process and preprocessing. In Section 4, we present a short introduction to Zernike moments, and provide a brief review of the algorithm for high-order Zernike moments computation. Feature extraction and matching are presented in Section 5 while experimental results and comparisons are presented in Section 6. Finally, Section 7 includes our conclusions and plans for future work.

2. Previous Work

The majority of hand-based verification systems using geometric measurements are based on research limited to considerably old patents [7] and commercial products. In these systems, the user is asked to place his/her hand on a surface and align it, with the help of some guidance pegs, on the surface. A mirror is usually used to obtain a side view of the hand using a single camera. The alignment operation simplifies the feature extraction process to a great extent and allows high processing speeds. In most cases, a few hand-crafted geometric features (e.g. length, width and height of the fingers, thickness of the hand, aspect ratio of fingers and palm . . . etc.) are extracted, making it possible to construct a small template (i.e., 9 bytes in some commercial systems).

Enhancing the ease of use and/or recognition accuracy of the system described above has drawn some attention only recently. Some studies have concentrated on accuracy only. Sanchez-Reillo et al. [17, 16] have proposed a new and richer set of geometric features and have investigated the use of multiple templates for an individual. Gaussian Mixture Models (GMMs) were employed to model each subject. Jain and Duta [6] proposed the use of the whole silhouette contour of the hand directly for alignment and matching.

Several studies have reported that peg-based alignment is not very satisfactory and represents in some cases a considerable source of failure [17, 7]. Although peg removal provides a solution to reduce user inconvenience, it also raises more challenging research problems due to the increase in intra-class variance. More recent studies [14, 22, 9, 4, 12, 24] have concentrated on the design of more convenient peg-free systems. Segmenting each finger and the palm in the silhouette image is usually the first processing stage in these systems. Once the fingers have been segmented, it becomes possible to extract and normalize geometric features [22, 9, 12], or contours [12, 24] for each part of the hand. Employing multiple templates is usually a requirement in peg-free systems [22, 9, 4].

Another important approach in the literature involves reconstructing the 3D surface of the hand. Woodard et. al [23] have used a range sensor to reconstruct the dorsal part of the hand. Local shape index values of the fingers were used as features in matching. In a related study, Lay et. al. [10] projected a parallel grating onto the dorsal part of the hand to extract features that indirectly capture 3D shape information.

3. Image Acquisition and Preprocessing

Our image acquisition system consists of a VGA resolution CCD camera and a planar lighting table, which forms the surface for placing the hand. The direction of the camera is perpendicular to the lighting table as shown in Fig. 1(a). The camera has been calibrated to remove lens distortion. It should be mentioned that, both the camera and the lighting table can be placed inside a box to completely eliminate light interferences from the surrounding environment; however, the current setting provides fairly high quality images without much effort from our side to control the environment. When the user places his/her hand on the surface of the lighting table, an almost binary, shadow and noise free, silhouette of the hand is obtained (see Fig. 1(b) and (c)). An alternative approach would be using a scanner to acquire the hand silhouette. During the acquisition process, users are just asked to stretch their hand and place it inside a large rectangular region marked on the surface of the table. This is to ensure the visibility of the whole hand and

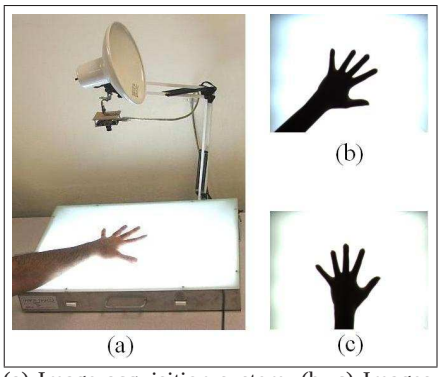

Figure 1. (a) Image acquisition system, (b, c) Images of the the same hand acquired by the system.

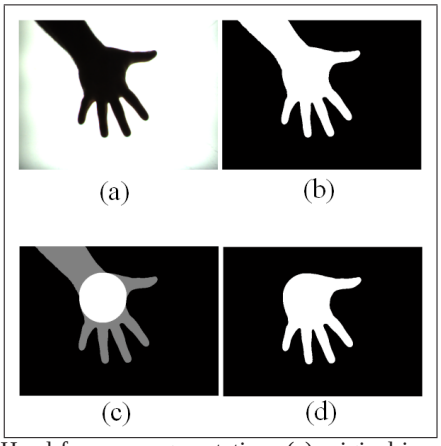

Figure 2. Hand-forearm segmentation: (a) original image, (b) binarized image, (c) largest circle inside the silhouette, and (d) segmented hand silhouette.

to avoid perspective distortions. There are no limitations on the orientation of the hand.

After the image has been captured, it is binarized to obtain the hand and forearm silhouettes. Due to the high contrast of the images obtained, simple thresholding gives high quality and accurate silhouettes as shown in Fig. 2(b). The next step involves separating the forearm from the hand. For this purpose, first we detect the palm by finding the largest circle inscribed in the hand-arm silhouette as shown in Fig. 2(c)). This process is fully automated and uses morphological operators. Then, the intersection of the forearm with the circle's boundary is found to segment the hand. Fig. 2(d) shows an example.

4. Zernike Moment Computation

Zernike moments are based on a set of complex polynomials that form a complete orthogonal set over the interior of the unit circle [25]. They are defined as the projection of the image on these orthogonal basis functions. Specifically, the basis functions $V_{n,m}(x,y)$ are given by

$$V_{n,m}(x,y) = V_{n,m}(\rho,\theta) = R_{n,m}(\rho)e^{jm\theta} \qquad (1)$$

where *n* is a non-negative integer, *m* is a non-zero integer subject to the constraints $n-|m|$ is even and $|m| < n$, ρ is the length of the vector from origin to (x,y) , θ is the angle between the vector ρ and the *x*-axis in a counter clockwise direction, and $R_{n,m}(\rho)$ is the Zernike radial polynomial. $R_{n,m}(\rho)$ is defined as follows:

$$R_{n,m}(\rho) = \sum_{k=|m|,n-k=even}^{n} \frac{(-1)^{\frac{n-k}{2}}\frac{n+k}{2}!}{\frac{n-k}{2}!\frac{k+m}{2}!\frac{k-m}{2}!}\rho^k = \sum_{k=|m|,n-k=even}^{n} \beta_{n,m,k}\rho^k \qquad (2)$$

The Zernike moment of order *n* with repetition *m* for a *digital* image function $f(x,y)$ is given by [8]:

$$Z_{n,m} = \frac{n+1}{\pi}\sum_{x^2+y^2\leq 1}\sum f(x,y)V^*_{n,m}(x,y) \qquad (3)$$

where $V^*_{n,m}(x,y)$ is the complex conjugate of $V_{n,m}(x,y)$. To compute the Zernike moments of a given image, the image center of mass is taken to be the origin.

A method to improve the speed of Zernike moments computation involves using a quantized polar coordinate system. In [13] and [5], a square to a circle transformation was employed for this purpose. In [3], for an $M \times M$ image, the angles were quantized to $4M$ and the radii were quantized to M levels. A side effect of quantization is that errors are introduced in the computation of high-order Zernike moments (see next Section).

In this work, we employ an improved algorithm reported in [2] which avoids using any quantization, therefore, the computation of the moments is as accurate as in the traditional approach (i.e., no approximations). To save computation time, this algorithm finds the terms that occur repeatedly in various orders and avoids recomputing. Further computations are saved by employing a look-up table. To ensure high accuracy, it uses arbitrary precision arithmetic. In the next subsection, we summarize the main ideas behind this algorithm and compare it with Belkasim's method, which has given the best reconstruction error among the fast implementations mentioned above.

4.1. Efficient High-Order Zernike Moment Computation

By substituting Eqs. 2 and 1 in 3 and re-organizing the terms, the Zernike moments can be computed as follows:

$$
\begin{aligned}
Z_{0,0} &= \beta_{0,0,0}\boxed{\chi_{0,0}} \\
Z_{2,0} &= \beta_{2,0,0}\chi_{0,0} + \beta_{2,0,2}\boxed{\chi_{0,2}} \\
Z_{4,0} &= \beta_{4,0,0}\chi_{0,0} + \beta_{4,0,2}\chi_{0,2} + \beta_{4,0,4}\boxed{\chi_{0,4}} \\
Z_{6,0} &= \beta_{6,0,0}\chi_{0,0} + \beta_{6,0,2}\chi_{0,2} + \beta_{6,0,4}\chi_{0,4} + \beta_{6,0,6}\boxed{\chi_{0,6}} \\
Z_{8,0} &= \beta_{8,0,0}\chi_{0,0} + \beta_{8,0,2}\chi_{0,2} + \beta_{8,0,4}\chi_{0,4} + \beta_{8,0,6}\chi_{0,6} + \beta_{8,0,8}\boxed{\chi_{0,8}} \\
Z_{10,0} &= \beta_{10,0,0}\chi_{0,0} + \beta_{10,0,2}\boxed{\chi_{0,2}} + \beta_{10,0,4}\chi_{0,4} + \beta_{10,0,6}\chi_{0,6} + \beta_{10,0,8}\chi_{0,8} + \beta_{10,0,10}\boxed{\chi_{0,10}}
\end{aligned}
$$

Figure 3. Common terms for computing Zernike moments up to order 10 with zero repetition.

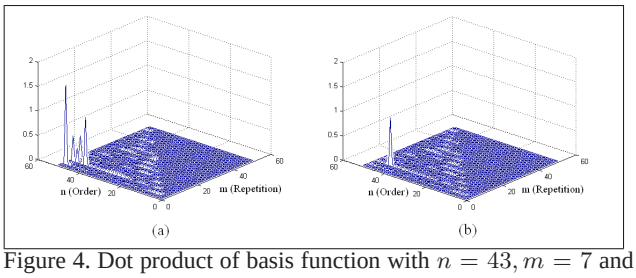

Figure 4. Dot product of basis function with $n = 43, m = 7$ and other basis functions up to order 50 using (a) double precision and (b) arbitrary precision arithmetic.

$$
\begin{aligned}
Z_{n,m} &= \frac{n+1}{\pi} \sum_{x^2+y^2 \le 1} \sum \Big(\sum_{k=|m|}^{n} \beta_{n,m,k} \rho^k \Big) e^{-jm\theta} f(x,y) \\
&= \frac{n+1}{\pi} \sum_{k=|m|}^{n} \beta_{n,m,k} \Big(\sum_{x^2+y^2 \le 1} \sum e^{-jm\theta} \rho^k f(x,y) \Big) \\
&= \frac{n+1}{\pi} \sum_{k=|m|}^{n} \beta_{n,m,k} \chi_{m,k} \qquad (4)
\end{aligned}
$$

The $\chi_{m,k}$'s defined in Eq. 4 become common terms in the computation of moments with the same repetition as shown in Fig. 3 for repetition m=0. In general, to compute Zernike moments up to order N, we would need to compute $\chi_{m,k}$ for each repetition. However, computing $\chi_{m,k}$ only once would be enough for computing Zernike moments of any order and any repetition by simply taking linear combinations as shown in Eq. 4. Moreover, the coefficients $\beta_{n,m,k}$ (see Eq. 2) do not depend on the image or the coordinates; therefore, they can be stored in a small look-up table to save computations [2].

Another important issue in high-order Zernike moment computation is numerical precision [2]. Depending on the image size and the maximum order, double precision arithmetic does not provide enough precision and serious numerical errors can be introduced in the computation of the moments. This fact is demonstrated in Fig. 4 by showing the effect of numerical errors on the orthogonality of the basis functions. As it can be observed in Fig. 4(a), obtained using double precision, orthogonality is violated seriously. Fig. 4(b), obtained using arbitrary precision arithmetic, shows that the orthogonality of the basis functions is preserved (i.e., only a delta function peak is present).

4.2. Comparison to Belkasim's Method

Our initial experimental results have indicated that accurate computation of Zernike moments is critical for our system to perform well. Here, we used the reconstruction error as a measure of accuracy:

$$
\varepsilon_r = \frac{\sum_x \sum_y |\tilde{f}(x,y) - f(x,y)|^2}{\sum_x \sum_y f(x,y)^2} \qquad (5)
$$

where $f(x,y)$ is the original image and $\tilde{f}(x,y)$ is the reconstructed image (up to order N)). Table 1 shows the reconstruction error of the method employed here and Belkasim's method using several different images and different orders. In implementing Belkasim's algorithm, we used arbitrary precision arithmetic to make a fair comparison. In general, it should be expected that the error decreases with increasing the order of Zernike moments. The method employed here illustrates such a behavior, however, Belkasim's method behaves quite differently which indicates that the quantization of polar coordinates has a serious effect on the computation of higher-order moments.

Table 1. Reconstruction error for a number of different images using our method and Belkasim's method.

Order	Our method	Belkasim's method
35	0.0647	0.0648
40	0.0621	0.0628
45	0.0596	0.063
50	0.0370	0.0557
55	0.0203	0.0645
60	0.0133	0.0665

Table 2 shows the number of multiplications and additions required by the method employed here and Belaksim's method for an $M \times M$ image and moments up to order N. Overall, both methods have the same computational complexity which is $O(N^2M^2)$ although Belaksim's method performs less additions.

Table 2. Computational complexity of different methods.

	Additions	Multiplications
Belkasim's method	$O(NM^2)$	$O(N^2M^2)$
Our method	$O(N^2M^2)$	$O(N^2M^2)$

5. Feature Extraction and Matching

An important parameter in our system is choosing the maximum order of Zernike moments. Liao et. al. [11]

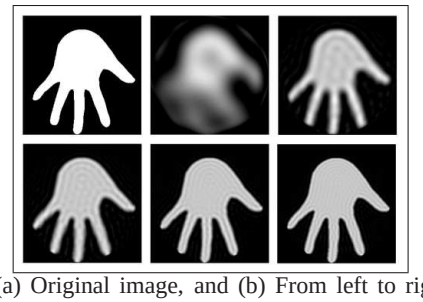

Figure 5. (a) Original image, and (b) From left to right, top to bottom, reconstructed images of original image up to order 10, 20, 30, 40, 50, 60, 70, 80 and 90, respectively.

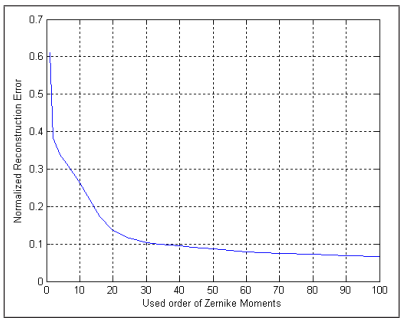

Figure 6. Reconstruction error on hand images.

showed that there is an inherent limitation in the precision of computing Zernike moments due to the circular geometry of the domain. Thus, arbitrarily high order moments are not accurate and useful for recognition. In this study, we used the average reconstruction error (see Eq. 5) on a large number of hand images to decide the maximum order in the context of our application. Fig. 6 shows the reconstruction error for different orders. As it can be observed, the error almost saturates for orders higher than 70. Fig. 5, shows the reconstructions for different orders. The saturation observed in Fig. 6 is also visually evident in Fig. 5. Based on these experiments, the maximum order chosen in our system was 70. Our experimental results justify this decision too.

Zernike moments up to order 70 yield a feature vector of 1296 components. To enable a smaller template size, PCA is used to reduce the dimensionality. Alternatively, feature selection could be used to choose a small subset of discriminant moments [18]. Using only 30 components, we were able to capture 99% of the information. For matching, we used the Euclidean distance. The resulting templates are translation, rotation, and scale invariant although scale invariance is not absolutely necessary in our application since the distance of the hand from the camera is fixed. Since we use multiple templates for each subject, our similarity criterion is based on the minimum distance between the query and the templates.

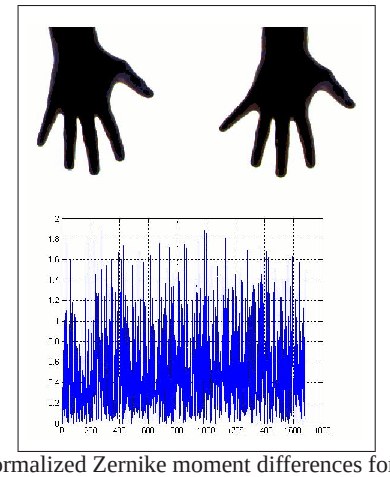

Figure 7. Normalized Zernike moment differences for two images of the same hand containing finger motion - less than 1.8% max error is shown.

6. Experimental results

In order to evaluate our system, we collected data from 40 people of different age and sex. For each subject, we collected 10 images of their right hand during the same session. Besides asking the subjects to stretch their hand and place it inside a square area drawn on the surface of the lighting table, no other restrictions were imposed as shown in Fig. 8). To capture different samples, subjects were asked to remove their hand from the lighting table, relax for a few seconds, and then place it back again. As a result, finger movements were unavoidable. For example, the middle and ring fingers are more apart from each other in Fig. 8(d) than in Fig. 8(c). Our experimental results show that Zernike moments can tolerate certain finger movement (e.g., 6 degrees rotation about the axis perpendicular to the joint of the finger with the palm), however, they are more sensitive when fingers move close to each other. Interestingly enough, finger motion does not affect high-order moments significantly more than low-order moments (see Fig. 7). Also, Zernike moments cannot tolerate very well situations where the hand is bent at the wrist. In our database, which contains 400 samples, the maximum distance between samples was 0.6556. The mean distance between samples of the same subject (i.e., 1800 pairs of hands) was 0.2063, while the mean distance between samples of different subjects (i.e.,76,200 pairs of hands) was 0.4507.

We used different number of samples (e.g., 3,4, and 5) for each subject as enrollment templates. To capture the effect of template selection on overall system performance, we repeated each experiment ten times, each time choosing the enrollment templates randomly. The remaining samples were used to construct matching and non-matching sets to estimate False Acceptance Rate (FAR) and False Reject Rate (FRR). Figs. 9, 10 and 11 show the average ROC

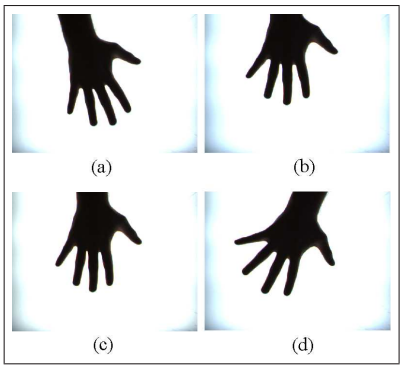

Figure 8. Sample images belonging to the same subject.

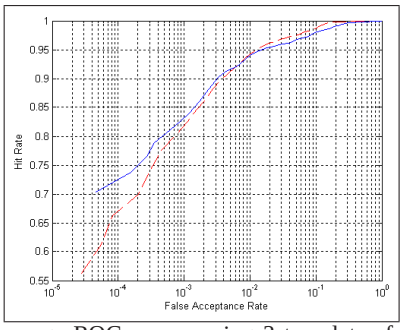

Figure 9. Average ROC curves using 3 templates for each subject; the solid and dashed curves correspond to the raw Zernike moments and PCA features respectively.

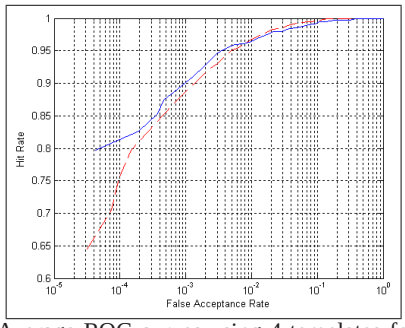

Figure 10. Average ROC curves using 4 templates for each subject; the solid and dashed curves correspond to the raw Zernike moments and PCA features respectively.

curves using 3, 4 and 5 templates per subject respectively. For comparison purposes, our tests were performed using both Zernike moments and PCA features.

Table 3 shows the mean and standard deviation of FRR when $FAR = 1\%$ using different number of templates. In all cases, performance was better using PCA was rather than using raw Zernike moments except for very low FAR values. Moreover, we obsereved that the error rates decrease to a great extent with an increase in the number of templates, which also enforces the use of PCA.

To further investigate the performance of our system, we have performed a qualitative comparison of the error rate

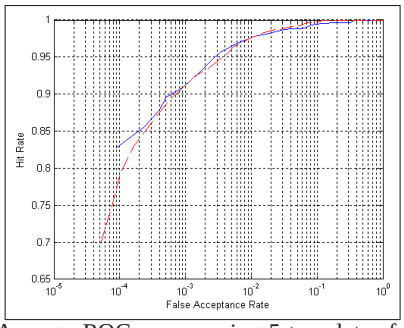

Figure 11. Average ROC curves using 5 templates for each subject; the solid and dashed curves correspond to the raw Zernike moments and PCA features respectively.

Table 3. Mean and standard deviation of FRR when $FAR = 1\%$.

No. of Training vectors	3	4	5
$\overline{FRR}$ (%)	6.03	3.56	2.44
σ_{FRR} (%)	2.09	1.80	0.67
$\overline{FRR}$ (%) [using PCA]	5.82	3.28	2.42
σ_{FRR} (%) [using PCA]	1.97	1.27	1.08

of our system and those reported in the literature (see Table 4, last row). Since there is no standard acquisition method and, as a result, no benchmark databases, comparing different systems on a qualitative way is difficult. To make the comparison more fair, for each study considered in our comparison, we are also reporting several other factors such as number of subjects, number of images per person, number of templates, use of pegs, type of features, and distance measures. The results reported for our system in Table 4, were obtained using 5 templates. From the table, it can be concluded that our system has comparable or lower error rates than any other system shown. In terms of systems using databases of comparable size to the one used in our experiments, the error estimates produced by our system are better than the first 5 systems reported in Table 4.

7. Conclusions and Future Work

We have presented a novel peg-free hand-based verification system using high order Zernike moments. To make the computation of high-order moments feasible, we presented a new algorithm that avoids redundant computations to speed up things and uses arbitrary precision arithmetic to ensure accurate moment computations. Using a database of 400 images from 40 subjects, the average error rate of our system using 5 templates was FRR=2.42% when FAR=1% and EER=2%. Qualitative comparisons between our system and other systems reported in the literature indicate that our system performs comparable or better.

It should be noted that our system is still under development and further work is required to improve its performance. First of all, to tolerate finger movement, espe-

cially movements of the middle finger, subjects were asked to stretch their hand prior to placing it on the lighting table. Although such a requirement does not cause any inconvenience to the subjects, an alternative approach would be segmenting the fingers and the palm. Then, verification can be performed by just considering information from the fingers, the palm or both. Such an approach would tolerate finger motion and completely remove the requirement to place the hand in a stretched position. Second, we plan to investigate the idea of combining multiple templates into a single, "super-template", to reduce memory requirements but also build more accurate models for each individual. Third, we plan to increase the size of the database in order to perform larger scale experiments and obtain more accurate error estimates. Moreover, we plan to test the robustness of the method when there is substantial passage time between the template and test images. Finally, we plan to compare our technique with other techniques using the same database to reach more useful conclusions.

Acknowledgments

This work was supported in part by NASA under grant # NCC5-583.

References

[1] Biometrics market and industry report 2004-2008. *http://www.biometricgroup.com/reports/public/market_report.html*.

[2] G. Amayeh, A. Erol, G. Bebis, and M. Nicolescu. Accurate and efficient computation of high order zernike moments. *First International Symposium, ISVC 2005, Lake Tahoe, NV, USA*, pages 462–469, December 2005.

[3] S. O. Belkasim, M. Ahmadi, and M. Shridhar. Efficient algorithm for fast computation of zernike moments. *IEEE 39th Midwest symposium on Circuits and Systems*, Vol. 3:1401 – 1404, 18-21 Aug. 1996.

[4] Y. Bulatov, S. Jambawalikar, P. Kumar, and S. Sethia. Hand recognition using geometric classifiers. *ICBA'04, Hong Kong, China*, pages 753–759, July 2004.

[5] J. Gu, H. Z. Shua, C. Toumoulinb, and L. M. Luoa. A novel algorithm for fast computation of zernike moments. *Pattern Recognition*, Vol. 35:2905 2911, 2002.

[6] A. Jain and N. Duta. Deformable matching of hand shapes for verification. *Proc. IEEE Int. Conf. on Image processing, Kobe, Japan*, pages 857–861, October 1999.

[7] A. Jain, A. Ross, and S. Pankanti. A prototype hand geometry-based verification system. *Proc. 2nd Int. Conf. on Audio- and video-based personal authentication (AVBPA), Washington, USA*, pages 166–171, March 1999.

[8] A. Khotanzad and Y. H. Hong. Invariant image recognition by zernike moments. *IEEE Transactions on Pattern Analysis and Machine Intelligence*, Vol. 12:489 – 498, 1990.

[9] A. Kumar, D. C. M. Wong, H. C. Shen, and A. K. Jain. Personal verification using palmprint and hand geometry biometric. *Time-Varying Image Processing and Moving Object Recognition, Guildford, UK*, pages 668–678, June 2003.

[10] Y. L. Lay. Hand shape recognition. *Optics and Laser Technology*, 32(1):1–5, Feb. 2000.

[11] S. X. Liao and M. Pawlak. On the accuracy of zernike moments for image analysis. *IEEE Transactions on Pattern Analysis and Machine Intelligence*, Vol. 20, No. 12:1358 – 1364, December 1998.

[12] Y. L. Ma, F. Pollick, , and W. Hewitt. Using b-spline curves for hand recognition. *Proc.of the 17th International Conference on Pattern Recognition (ICPR'04)*, Vol. 3:274–277, Aug. 2004.

[13] R. Mukundan and K. Ramakrishnan. Fast computation of legendre and zernike moments. *Pattern Recognition*, Vol. 28,No. 9:1433 1442, 1995.

[14] S. Ribaric, D. Ribaric, and N. Pavesic. Multimodal biometric user-identification system for network-based applications. *IEE Proceedings on Vision, Image and Signal Processing*, Volume 150, Issue 6:409–416, 15 Dec. 2003.

[15] A. Ross and A. Jain. Information fusion in biometrics. *Pattern Recognition Letters*, 24(13):2115–2125, 2003.

[16] R. Sanchez-Reillo. Hand geometry pattern recognition through gaussian mixture modelling. *15th International Conference on Pattern Recognition (ICPR'00)*, Volume 2:937–940, 2000.

[17] R. Sanchez-Reillo, C. Sanchez-Avila, and A. Gonzalez-Marcos. Biometric identification through hand geometry measurements. *IEEE Transactions on Pattern Analysis and Machine Intelligence*, Vol. 22, No. 10:1168–1171, October 2000.

[18] Z. Sun, G. Bebis, and R. Miller. Object detection using feature subset selection. *Pattern Recognition*, 37:2165–2176, 2004.

[19] M. R. Teague. Image analysis via the general theory of moments. *J. Opt. Soc. Am.*, Vol. 70,Issue. 8:920 930, 1980.

[20] C. Teh and R. Chin. On image analysis by the methods of moments. *IEEE Transactions on Image Analysis and Machine Intelligence*, 10(4):496–513, 1988.

[21] C. H. Teh and R. T. Chin. On image analysis by the method of moments. *IEEE Transactions on Pattern Analysis and Machine Intelligence*, Vol. 10:485 513, 1988.

[22] L. Wong and P. Shi. Peg-free hand geometry recognition using hierarchical geometry and shape matching. *IAPR Workshop on Machine Vision Applications, Nara, Japan*, pages 281–284, 2002.

[23] D. L. Woodard and P. J. Flynn. Personal identification utilizing finger surface features. In *CVPR*, San Diego, CA, USA, 2005.

[24] W. Xiong, C. Xu, and S. H. Ong. Peg-free human hand shape analysis and recognition. *Proc. of IEEE International Conference on Acoustics, Speech, and Signal Processing (ICASSP '05)*, Volume 2:77–80, March 18-23 2005.

[25] F. Zernike. *Physica*. 1934.

Table 4. Quick reference of existing methods.

System(s)	# of people	# of Sample per person	Pegs	# of Template(s)	Feature(s)	Similarity	Performance
Jain [7]	50[1]	10	Yes	2	Geometric features[11] (16 features)	Mahalanobis	FAR=0.01 FRR[2]≈0.17
Wong [22]	22[3]	12-15	No	9	13 geometric features[11] and 3 fingertip regions	GMM	FAR=0.022 FRR=0.1111
Jain [6]	53[4]	2-15	Yes	1[5]	Contour of five fingers	Max. Abs. Error	FAR=0.01 FRR[2]≈0.06
Reillo [17][16]	20	10	Yes	5	Geometric features[11] deviation and angles between the inter-finger points (25 features)	Euclidean Hamming GMM	EER[8]=0.049 error rate[6]≤0.1
Ma [12]	20	6	No	1	4 B-Spline curves, length of thumb and width of palm	see [12]	error rate=0.05
Kumar [9]	100	10	No	5	Geometric features[11] and hand area (16 features)	Correlation Coeff.	FAR=0.01 FRR[9]≈0.32
Bulatov [4]	70[7]	10	No	5	30 geometric features[11]	Nearest Box	FAR=0.01 FRR=0.03
Ribaric [14]	130	5	No	1	20 geometric features[11]	Euclidean	FAR=0.153 FRR[10]=0.13
Xiong [24]	108	5	No	1	Width of 4 fingers at 45 different location for each one	see [24]	EER=0.0241
Our method	40	10	No	5	Zernike moments (30 PCA features.)	Euclidean	FAR=0.01 FRR=0.0242 EER=0.0164 error rate[6]=0.0326

1. Out of 500 images, 140 images were discarded and only 360 images were used.
2. Estimated from ROC curve in [7].
3. A total of 288 images were used.
4. A total of 353 images were used.
5. Not all possible non-matching pairs were used.
6. The minimum error rate, which is the sum of FAR and FRR.
7. A total of 714 images were used.
8. This is the best EER using 5 training vectors and GMM for verification [16].
9. Hand geometry was used to improve the performance of palmprint-based verification. We have estimated FRR using only hand geometry information from the ROC curve in [9] when FAR=0.01.
10. A multi-modal biometric system was designed in [14] using fingerprint, palmprint, and hand geometry. The FAR and FRR reported here relates to hand geometry only, see [14].
11. Geometric features such as length and width of the fingers, width of palm, thickness of hand and middle finger, etc.